7 Pathologic Rationale for Focal Therapy of Prostate Cancer: Elucidating Tumor Characteristics and Biology

Vladimir Mouraviev, Arnauld Villers, Thomas M. Wheeler, Rodolfo Montironi, Pierre Nevoux, Ariel Schulman, and Thomas J. Polascik

Introduction

The contemporary widespread detection of early-stage prostate cancer (PCa) has led to a dramatic shift in the treatment paradigm of localized disease toward nonaggressive and minimally invasive approaches such as active surveillance (AS) and focal therapy (FT) [1–3]. Quality of life outcomes, in particular urinary continence and erectile function, are particularly important to the relatively young cohort of men in their fifties and sixties who are candidates for PCa treatment. During the last several decades, pathologic and clinical studies have been done to better understand the role of prostate-preserving ablative technologies using targeted ablation as a "male lumpectomy" in appropriate candidates [4–8].

The recognition of the multifocality of the majority of cases of PCa, likelihood of synchronous cancer lesions, and lack of specific and sensitive imaging modalities to accurately identify the extent or contours of significant cancer foci remain major limitations to more broad implementation of FT [9–11]. Although, several recent studies based on unbiased genome-wide approaches demonstrated that anatomically distinct tumor metastases are derived from a single progenitor clone [12–15]. These data of the literature suggest that most commonly the driver lesion with potentially lethal clone is located inside of the index focus, which gives the bright prospects for focal ablation of this focus with potentially curable intent. However, currently, we still lack a reliable diagnostic tool to rule out an existence of this lethal clone in secondary (satellite) lesion(s) in some cohort of patients.

V. Mouraviev (✉)
Central Florida Cancer Institute, Davenport, FL, USA
e-mail: Vladimir.Mouraviev@flhosp.org

A. Villers
Department of Urology, Hôpital Huriez, Centre Hospitalier Regional Universitaire, Université Lille Nord de France, Lille, France

T.M. Wheeler
Department of Pathology and Immunology, Baylor College of Medicine, Houston, TX, USA

R. Montironi
Department of Pathology, Genitourinary Cancer Program, Institute of Pathological Anatomy and Histopathology, Polytechnic University of the Marche Region (Ancona), School of Medicine, United Hospitals, Torrette, Ancona, Italy

P. Nevoux
Department of Urology, Regional University of Lille, Lille, France

A. Schulman
Duke Cancer Institute and Department of Surgery, Duke University Medical Center, Durham, NC, USA

T.J. Polascik, MD
Professor of Surgery, Division of Urology, Department of Surgery, Duke Cancer Institute, Duke University School of Medicine, Durham, NC, USA

T.J. Polascik (ed.), *Imaging and Focal Therapy of Early Prostate Cancer*, Current Clinical Urology, DOI 10.1007/978-3-319-49911-6_7

In this chapter we review the current literature on the pathologic significance of PCa including a number of tumors, location, aggressiveness, invasiveness, uni- vs. multifocality, and laterality along with genomic alterations. As we continue to understand the histologic and genomic biology of index and satellite lesions, we can better select candidates and predict those men most likely to benefit from an organ-preserving treatment approach.

The Pathological Parameters Defining Clinically Significant Prostate Cancer and Rationale for Focal Therapy

An international consensus panel of experts recently provided guidance on patient eligibility, interventions, and meaningful outcome measures for FT in clinical practice [16]. The panel noted a trend toward including FT for intermediate-risk disease compared to previously existing approaches treating only men with low-risk disease. This shift is based on growing confidence in the technique and promising medium-term follow-up results of multiple clinical trials [17–20]. Some critical definitions for patient selection were revised according to new data. For instance, prostate volume should no longer be a primary determinant of eligibility for FT. Other factors that require consideration include tumor grade and the boundaries and morphologic characteristics of the lesion. Furthermore, there are limitations in different ablative modalities that should be considered in planning focal therapy [16]. For example, high-intensity focused ultrasound (HIFU) may not have the required focal length to reach anterior lesions in larger glands.

The Index Lesion as a Driver of Cancer Progression

There are multiple factors including multifocality and varied histological, genomic, and molecular abnormalities that determine whether PCa will behave in an indolent or aggressive fashion. More than 80 % of prostatectomy specimens contain more than one disease focus [21, 22]. The index tumor, or dominant lesion, is defined as the largest volume lesion and presumed to be the main determinant for tumor progression and prognosis. Unifocal cancer has been identified in 13–33 % of radical prostatectomy (RP) specimens, and is generally associated with lower grade, stage, and recurrence rates than multifocal cancers [23–26]. In a review by Mouraviev et al., histologic features of the index lesion were linked to prostate cancer follow-up and generally were the main determinant of prognosis [4]. Karavitakis et al. reported that the largest lesion usually contains the worst histologic features on radical prostatectomy specimen [27]. This was confirmed by Huang et al. who analyzed 201 specimens and noted that the largest tumor volume, highest Gleason score (GS) and extraprostatic extension (if present) occurred within the same lesion in 88.7 % of cases with multifocal disease [28].

In the index lesion hypothesis, the satellite lesions, or secondary foci, are thus considered to be non-life-threatening. This is supported by a contemporary study by Mizuno et al. who reported that the largest tumor was a predictor of recurrence after treatment at multivariate analysis, alongside Gleason score and positive surgical margin [29]. Indeed, Liu et al. reported an autopsy series that noted a monoclonal cell precursor as the origin of metastasis [13]. Similarly, Mehra et al. described a single origin of metastasis [14]. Ding et al. found that some specific genetic alterations have implications in prostate cancer growth and metastatic progression [30]. Ultimately, Ahmed et al. formalized the concept of the index lesion according to data suggesting that genomic "signatures" of PCa and its metastases are all derived from a single clone in the prostate gland [31].

Based on 222 men with stage T1c PCa treated with RP, Noguchi et al. studied the prognostic value of secondary cancers in men having multifocal, localized PCa [32]. The cohort was divided into three groups including men with a single tumor (54 cases, 24 %), an index tumor with secondary cancers <0.5 cc (86 cases, 39 %), and an

index tumor with secondary cancers >0.5 cc (82 cases, 37 %). On multivariate analysis of the three groups, the investigators did not detect any differences in preoperative prostate-specific antigen (PSA), number of positive cores, percent of Gleason grade 4 or 5 in the needle biopsy, or histological features in RP specimens. However, when analyzing PSA failure rates among the three groups, the group with an index lesion and smaller secondary cancers had a better prognosis than the group with a single tumor. This study suggests that patients with multifocal PCa do not necessarily have a worse outcome than men with unifocal lesions. A report by Haffner et al. studying 108 RP specimens suggested that secondary cancers are rarely significant in volume [33]. Two simultaneous, significant volume cancers >0.5 cc were identified in only 11 of 152 (7 %) cases.

The Role of Small Satellite Lesions: Do They Need to be Treated?

Several reports contend that secondary, small-volume tumors do not significantly influence the survival of patients after RP [34–37]. A study by Liu et al. revealed support for a single aggressive lesion affecting the mortality of patients with advanced PCa [13]. This multi-institutional study using high-resolution, genome-wide single nucleotide polymorphism and copy number reported on 94 anatomically separate cancer sites in 30 men who died from metastatic PCa. These data in conjunction with a single-locus genetic study of advanced PCa evaluating the role of TMPRSS2-ETS in tumor progression demonstrated that in spite of common genetic heterogeneity in primary cancers, most metastatic cancers arise from a single clone of index lesion [13].

On the contrary, emerging data suggests that secondary tumors may grow and become clinically significant over time [38, 39]. The advanced genome-wide association studies (GWAS) have emerged as a new approach to identify alleles associated with prostate cancer risk in unbiased fashion; i.e., without prior knowledge of their position or function [40–43]. These GWASs can shed light to better understand tumor subclonality by using spatio-genomic approaches and sequencing multiple foci from each individual patient. All studies demonstrated the presence of multiple independent cancer clones both within and between (intrapatient heterogeneity) suggesting that FT for prostate cancer may be complicated by heterogeneous molecular aberrations.

Haffner et al. tracked the evolution of the lethal cell clone from primary PCa to metastases through samples collected during disease progression and at the time of death over a 17-year treatment course following primary radical prostatectomy [38, 39] (Fig. 7.1a, b). Despite being limited to one case, these analyses demonstrated that the lethal clone arose from a small, relatively low-grade cancer focus with a Gleason grade of 6 in the primary tumor, and not from the bulky, higher-grade primary cancer of Gleason grade 7 or from a lymph node metastasis resected at prostatectomy.

Taken together, the aforementioned studies reveal a series of unexpected characteristics of localized prostate cancer. First, they demonstrate the presence of widespread field effects, with mutational stress across the entire prostate gland superimposed with tumor evolution and selective pressures to produce substantial spatial heterogeneity. Second, they highlight the challenge of treating tumors composed of different subclones, some of which may respond to specific systemic or targeted therapies, and suggest a need for multimodal interventions. Finally, they suggest that genomic interrogation of a single biopsy specimen may be insufficient to generate robust predictions from molecular biomarkers, even if suspected trunk mutations are considered because of apparent multiple clonally independent tumors within a single individual. To date, these conclusions are based on a limited number of patient trials; therefore they cannot be used to make generalizations for all candidates for FT. More robust clinical observations are required. Furthermore, it is well known that these multiple genetic events may not always have an impact on the natural history of the disease.

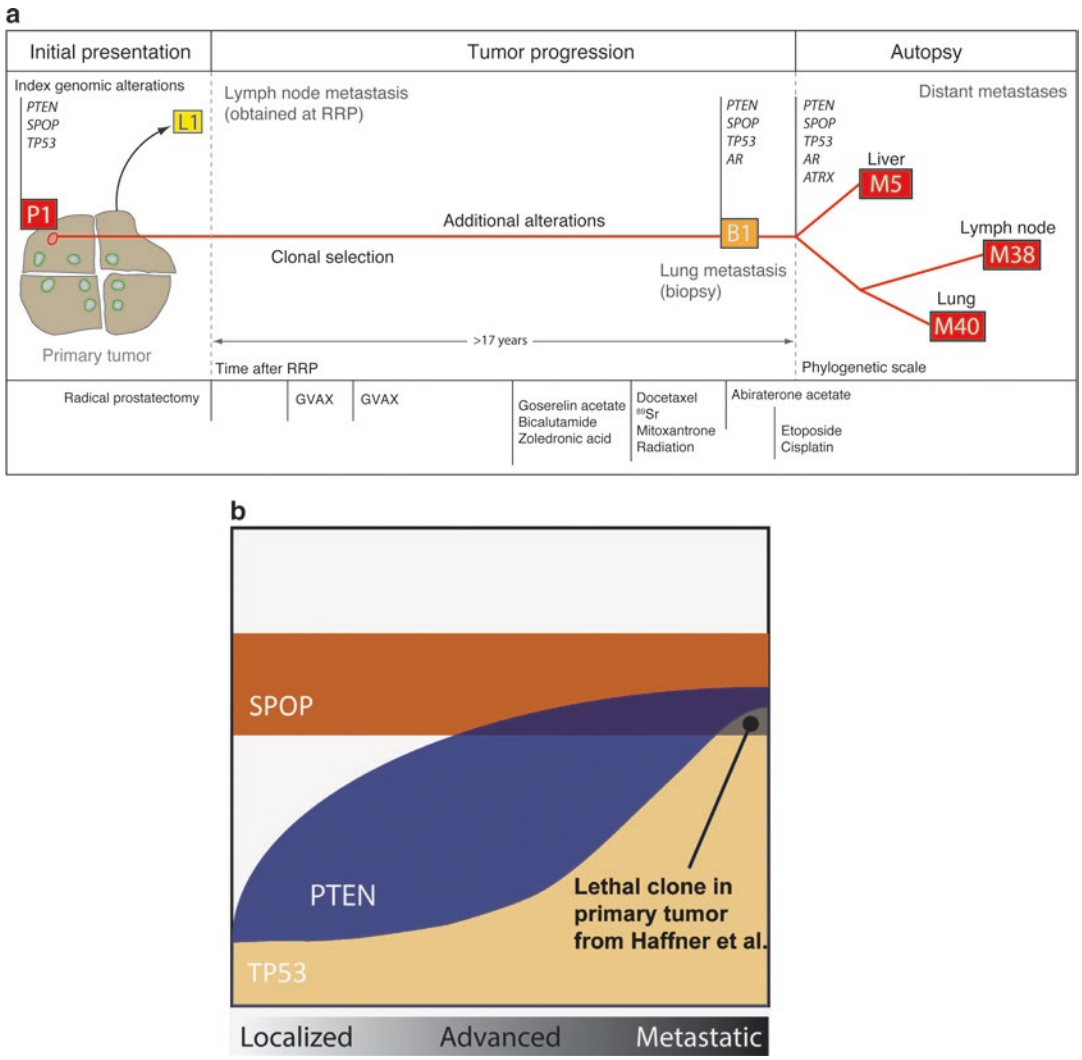

Fig. 7.1 Molecular and pathological findings in the primary tumor and their clonal relationship to the distant metastases. (**a**) Proposed model of disease progression in this index case, based on sequencing and molecular pathological analyses. Phylogenetic relationships of distant metastases were calculated based on structural rearrangements. (Reprinted with permission from Haffner MC, Mosbruger T, Esopi DM, Fedor H, Heaphy CM, Walker DA, et al. Tracking the clonal origin of lethal prostate cancer. J Clin Invest. 2013 Nov;123(11):4918–4922. [39]). (**b**) Speckle-type POZ protein (SPOP), phosphatase and tension homolog (PTEN), and tumor protein 53 (TP53) abnormalities across the spectrum of early and advanced prostate cancer. Reprinted with permission from Barbieri CE, Demichelis F, Rubin MA. The lethal clone in prostate cancer: Redefining the index. Eur Urol. 2014 Sep.;66(3): 395–397 [38]

If secondary cancers are initially left untreated, a stringent surveillance protocol including imaging and novel genomics tools should be followed. If significant growth of secondary lesions is noted during follow-up after index ablation, repeat ablation should be performed.

The index lesion may be considered the driving force of PCa progression and therefore should be identified and treated at an early stage. The majority of satellite lesions generally do not appear to be life threatening to the patient. Therefore, for patients considering FT, precise three-dimensional (3D) mapping biopsies and/or imaging studies should be done to identify and map the index tumor and ensure that potential clinically significant small-sized lesions are not inadvertently missed.

Cancer Laterality and Unifocality

Conventional PCa treatment, namely, whole-gland therapy, is dogmatically founded upon the principle of tumor heterogeneity and multifocality seen in 50–87 % of cases [4, 21, 22]. With prevalent PSA screening and early detection programs, investigators are now reporting an increased proportion of unifocal and/or unilateral disease.

Bostwick et al. demonstrated that multiple foci of prostatic intraepithelial neoplasia (PIN) may independently arise from various sites of the same prostate suggesting a field effect underlying the development of PCa [44]. Aurora et al. and Cheng et al. sequentially demonstrated that multifocal PCa is common (87 %) with extensive histological heterogeneity seen among foci within the same specimen even with very low total tumor volume [35]. These findings also support the "field effect" of carcinogenesis. Recently, the same group reviewed records of 184 patients with unifocal tumors [23]. They found that despite a number of patients with insignificant disease, the relative proportion of patients with a unifocal tumor increased from 13 % to 28 % in the overall cohort. Tumor focality failed to show an advantage in biochemical recurrence between unifocal and multifocal disease. There were not significant differences in 5-year biochemical recurrence-free survival (66 % and 61 %, respectively). However, these data suggest that unifocal lesions can be aggressive and require ablative therapy.

Some investigators found a significant difference in treatment outcome between unifocal and multifocal lesions [45], whereas others demonstrated that the number of tumor foci, index tumor volume, satellite tumor volume, or tumor unilaterality did not predict disease-free survival on multivariate analysis [32, 46, 47]. Such conflicting data suggest the limitations of single-institutional studies with specific geographic and demographic features along with variable follow-up. It also implies our incomplete knowledge about the natural history of early-stage disease, including the complexity of tumor biology and limited predictability of clinical behavior.

It has been noted that even within the same institution (Stanford, Colorado, and Indiana University, etc.) the incidence of unifocal PCa has fluctuated over time [25]. Some countries have shown a greater prevalence of unifocal lesions, such as Austria and France (30–33 %), and South Korea (67 %) based upon prostatectomy specimens [4]. This may reflect differences in selection factors, patient populations, and methods of tissue sampling, among other possible explanations.

From its onset, FT has encompassed the concept of hemi-ablation; e.g., ablating the side of the prostate containing the dominant or index tumor along with any other satellite lesions that are found on the same side of the prostate. Based upon this premise, the concept of the unilateral cancer may be a more practical approach than targeting the unifocal tumor. Mouraviev et al. analyzed 1186 prostatectomy specimens from patients with low- to low-intermediate risk, clinically localized PCa [48]. Pathologic assessment focused on cancer laterality, percentage of tumor involvement (PTI), and pathologic Gleason score. Unilateral cancer was identified in 227 (19.2 %) cases, suggesting that almost one of five candidates treated with surgery in contemporary series may be amenable to focal hemi-ablation of one side of the prostate.

It is important to recognize that there may be residual disease on the untreated side after hemi-ablation. Although small volume lesions are generally unilateral, some clinically significant tumors could be located on the contralateral side. Yoon et al. evaluated the contralateral gland in patients presumed to have unilateral prostate cancer on biopsy [49]. In this study of 100 low-risk patients, needle biopsy predicted what the authors defined as limited disease (less than 3 unilaterally positive cores, <50 % involvement of any positive core, Gleason score <6). Clinical stage T1c disease was diagnosed in 85 cases with cT2a disease in 15 with the palpable lesion located on the same side as the positive biopsies. In 66 cases, there was only one PCa focus identified in the contralateral lobe. Approximately 14 % of each positive core was involved with PCa. In 65 RP specimens, cancer was identified contralateral to the positive

biopsy side with a mean total tumor volume of 0.2 cm^3 (largest 1.3). There were 13 cases in which more than 0.5 cm^3 cancer was identified contralateral to the positive biopsy and seven with predominantly anteriorly located tumor. Overall, clinically significant cancer (Epstein definition) would have been missed in 20 % of cases in the contralateral lobe if hemi-ablation were performed based upon routine preoperative evaluation with *sextant* biopsy. This study underscores the limited accuracy of conventional, office-based transrectal ultrasound (TRUS)-guided prostate biopsy to select patients for hemi-ablation. In a study of 538 patients with biopsy-proven unilateral disease, analysis of the contralateral gland revealed pathologic features in 24 % of cases including extraprostatic extension (EPE) (14.9 %), PTI > 15 % (8.4 %), GS > 7 (4.7 %), seminal vesicle invasion (SVI, 2.5 %), or a combination of the aforementioned.

Bott et al. studied 100 prostatectomy specimens including men with intermediate- and high-risk disease and found multifocal disease in 84 patients, with 36 of them having had significant secondary tumors [50]. These clinically significant satellite cancers were defined by volume (≥0.5 ml), by grade (any Gleason pattern ≥4) in 19, and by stage (ECE) in six cases.

In the first prospective study from University College London, Ahmed et al. studied the feasibility of treating only the largest and highest-grade cancer in men with more than 1 known prostate tumor [51] (Fig. 7.2). They showed that the side effects of targeted ablation were low, with acceptable rates of early cancer control. The median PSA nadir decreased to 2.4 ng/ml (IQR 1.6–4.1). At 12 months, 42 of 52 (80.8 %) patients had histological absence of clinically significant cancer and 48 of 56 (85.7 %) patients had no measurable prostate cancer on rebiopsy or multiparametric magnetic resonance imaging (mpMRI). Despite an overall absence of clinically significant disease (primary end point) noted on follow-up, 43 % of men had persistent Gleason 6 disease at the study end. These cancers must be followed prospectively given the recent findings of Haffner et al. that noted distant metastasis originating from Gleason score 6 disease.

Gleason Grade

The Gleason grade reflects architectural patterns of groups of cancerous glands and has been established as an important predictor of biochemical and systemic failure as well as cancer-specific and overall survival. The new 2016 World Health Organization (WHO) Classification of PCa was recently introduced with a reorganized scoring system [52, 53] (Table 7.1). Gleason scores 2 to 6 are now condensed into a single prognostic grade group (PGG) 1, Gleason score 7 is divided into 2 groups based on primary score, and Gleason scores 9 and 10 are combined into group 5.

The international panel on FT agreed it was acceptable not to treat PGG 1 lesions up to a maximum cancer core length of 5 mm, although it has to be noted that the level of consensus was higher for not treating lesions with a smaller maximum cancer core length of 3 mm [16]. The panel agreed that PGG 2 (Gleason 3+4) lesions with a maximum cancer core length of 5 mm or PGG 3 (Gleason 4+3) disease of any length should be treated. However, the panel did not reach consensus on whether PGG 2 lesions with a maximum cancer core length of 3 mm could be left untreated.

In a contemporary series of patients who were selected for FT, most (85 %) had Gleason scores 5–7. Among these, Gleason 7 is of particular interest due to the controversy related to tumor biology and aggressiveness [17]. Some studies did not demonstrate a significant difference between clinical outcomes with histologically confirmed PGG 2 (GS 3+4) compared to PGG 3 (GS 4+3) disease [17]. However, other studies purport that cancers with primary Gleason pattern 4 have less favorable clinical behavior than those with primary Gleason pattern 3 [17]. Analyzing 1688 men 10 years after RP, Tollefson et al. demonstrated that a PGG 2 (GS 3+4) was associated with an increased biochemical disease-free survival (bDFS) (48 % vs. 38 %), lower systemic recurrence (8 % vs. 15 %), and higher cancer-specific survival (97 % vs. 83 %) compared to PGG 3 (GS 4+3), respectively [54]. Burdick et al. presented the results of 705 patients with Gleason

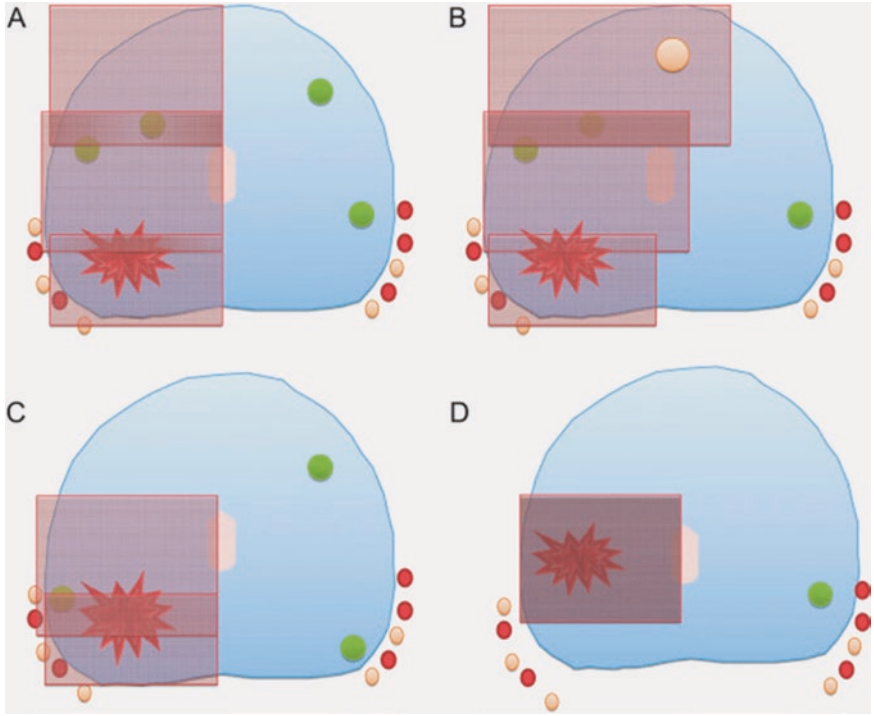

Fig. 7.2 Schematic diagrams demonstrating the types of focal therapy conducted in prospective development study on focal ablation of index lesion in multifocal localized prostate cancer. *Large red areas* represent dominant cancers (so-called index lesions), while *small green areas* represent small, low-grade, secondary lesions. *Red transparent boxes* represent ablation zones on the high-intensity focused ultrasound device: (**a**) hemi-ablation, (**b**) extended (dogleg) ablation, (**c**) quadrant ablation, (**d**) focal ablation. Reprinted with permission from Ahmed HU, Dickinson L, Charman S, Weir S, McCartan N, Hindley RG, et al. Focal ablation targeted to the index lesion in multifocal localized prostate cancer: a prospective development study. Eur Urol. 2015 Dec; 68(6):927–36

Table 7.1 World Health Organization (WHO) classification of prostate cancer

Prognostic grade group	Gleason score
1	3+3 = 6
2	3+4 = 7
3	4+3 = 7
4	8
5	9–10

7 prostate cancer treated with RP (n = 310), external beam radiotherapy (n = 268), or brachytherapy (n = 127) [55]. The 5-year bDFS rate was 78 % and 71 % (p = 0.0108) for PGG 2 (GS 3+4) and PGG 3 (GS 4+3), respectively [55]. The Physicians' Health Study and the Health Professionals Follow-Up Study reported on the mortality of PCa [56] suggesting that PGG 3 (GS 4+3) cancers were associated with a threefold increase in lethal PCa compared with PGG 2 (GS 3+4) cancers after RP.

Extraprostatic Extension Is Not an Absolute Contraindication to Focal Therapy

The risk of extraprostatic extension (EPE), which upgrades primary PCa to clinical stage T3a, should be considered in planning FT. EPE is a significant pathological parameter identified after RP that can influence disease-free recurrence. In a multivariate analysis by Ohori et al. the amount of EPE or prostate capsule invasion (PCI) was an independent prognostic factor of disease recurrence. These authors detected a strong correlation between the level of PCI and total tumor volume, Gleason grade, SVI, positive lymph node status

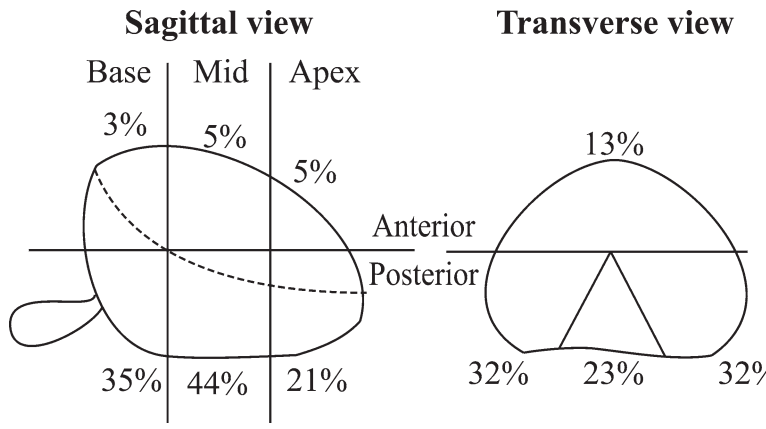

Fig. 7.3 Location and frequency of extraprostatic extension in radical prostatectomy specimens. Adapted from Ohori M, Scardino PT. Localized prostate cancer. Curr Probl Surg. 2002 Sep.;39(9):833–957 [57]

(+LN), and rate of biochemical recurrence after RP [57]. Of interest, PCa did not appear to metastasize in the absence of invasion into the prostate boundary regardless of the volume or grade of the intraprostatic tumor. Since EPE was identified as occurring more commonly on one side (85 % unilateral EPE vs. 15 % bilateral in this study), it is essential for optimal FT planning to understand the precise location of EPE. Unfortunately, EPE usually occurred near the neurovascular bundle (NVB) where it was exceedingly difficult to prevent collateral damage to this structure during thermal ablation. Figure 7.3 depicts the spatial location of EPE based on a large RP series from Baylor College of Medicine [57]. This map of possible locations of EPE is important and may guide treatment planning to preserve the contralateral NVB on the untreated side, thereby preserving erectile function.

Baylor and Memorial Sloan Kettering investigators studied the pathology of 1000 RP specimens of early-stage PCa patients [57]. The frequency of unifocal disease in men with baseline PSA <10 ng/ml was found to be 18 %. Generally, the largest (index) focus of cancer represented 80 % of the volume of all cancer present. They found that the index cancer was almost always the largest and highest-grade focus. However, in certain cases, larger lower-grade cancers were noted in the transition zone with smaller high-grade cancer in the peripheral zone. In these instances, the index cancer is defined as the one with the highest grade. Of 470 patients with PSA levels between 4 and 10 ng/ml, 30 % had EPE with 92 % of these derived from the index lesion, 5 % from more than one focus, and 3 % from smaller foci only. Of 126 patients with serum PSA ≤4 ng/ml, 20 % had EPE, 92 % of which emanated from the largest cancer and the remaining 8 % from other foci only. These data support the rationale to target the index lesion whereby the tumor burden would be reduced by 80 % and the focus giving rise to EPE would be controlled in >90 % of patients. Mouraviev et al. reported that among 1184 patients with low-risk PCa, EPE was noted in 19.2 % of RP specimens [48]. The majority of patients with EPE may still benefit from FT since several technologies such as cryoablation can extend beyond the capsule thereby treating EPE. However, this requires accurate identification of the location and extent of EPE and targeting the region accordingly during therapy.

Because EPE is a critical pathologic parameter of the natural history of carcinogenesis and prognosis, the curative intent to extend an ablative zone beyond the capsule is feasible, particularly when the index lesion is located near the capsule. Several ablative technologies can be used to safely destroy an index lesion with EPE with no collateral damage.

The Role of Spatial Distribution of Cancers According to Zone of Origin and Volume

An understanding of the modeling of cancer morphology such as the zonal origin and possibly intraprostatic patterns of cancer dissemination at histopathology is available for imaging interpretation and treatment planning. These models may help determine cancer volumes that can be followed as active surveillance or targeted by focal ablation. Additionally, planning may identify those cancers in which ablative therapy may affect areas of the prostate that are important for preservation of continence and potency. Combining histological data from RP sections, 12-core biopsy results, mpMRI data, and knowledge of the morphology of zonal prostate anatomy, it was possible to model PCa of different volumes and create graphical depictions of the likely shapes and sizes of tumors in different histological parts of the prostate, including modeling in axial versus coronal projections. Modeling studies estimate that approximately 30 % of low-volume cancers are located anteriorly. Anterior cancers originate in the transition zone (TZ) and may be compressed further anteriorly during benign prostatic hyperplastic (BPH) growth, giving rise to cancers located in the anterior fibromuscular stoma (AFMS).

A widely accepted tumor mapping strategy based on a 39-sector zone diagram from multiparametric MRI findings has been introduced by the recent European Society of Urogenital Radiology (ESUR) consensus meeting and modified by the American College of Radiology [58]. A prostate segmentation model defining each of the unique regions of the prostate for localization is depicted by Villers in chapter 28 of this book (see Fig. 28.2).

In a series of 108 RP specimens, Haffner et al. stated that of 188 peripheral zone (PZ) cancers, 179 were <4 cc and 168 were <2 cc [33]. PZ cancers tend to remain confined to their zone of origin for tumor volumes <2 cc. Between 2 cc and 4 cc, some cancers partly spread into the TZ or AFMS. In total, 64 % and 90 % of PZ cancers <4 cc were located in the lower and posterior half of the gland, respectively. Additionally, 10 % were located in the anterior horn of the PZ. Cancers <2 cc were confined to 1 lobe in 164 of 168 (98 %) cases and not confined in 3 of 11 (27 %) cancers measuring 2–4 cc in volume. Only cancer ≥2 cc involved both apex and base in the sagittal plane.

Bouye analyzed a series of 91 prostates with TZ/AFMS foci. Overall, 79 foci were <4 cc and 69 were <2 cc [59]. Additionally, 50 % and 70 % of cancers <4 cc were located in the anterior third and inferior half of the TZ and/or AFMS, respectively. The authors subclassified three varieties of the small cancers <2 cc according to their locations related to the boundaries of the histological zones: TZ type 1 (40 %) represented cancers confined to one TZ lobe; TZ type 2 (35 %) represented cancers mostly in one TZ lobe but crossing its anterior boundary; and type 3 AFMS (25 %) represented cancers confined to the AFMS.

Nevoux et al. analyzed a series of cystoprostatectomy specimens performed for bladder cancer from 345 consecutive patients without clinically manifested prostate cancer [60]. In the 96 prostates with prostate cancer, 215 cancer foci were identified (mean 2.24 cancers per prostate). Of the 215 cancers, 90 % were <0.5 cc and 79 % < 0.2 cc (Fig. 7.4). Overall, 88 % of cancer foci were clinically insignificant with a tumor volume <0.5 cc and no Gleason grades 4–5 (groups 4–5) (Fig. 7.5). Seventy-five percent of the cancer foci were located in the peripheral zone, while the remainder were within the transition zone. One-third of cancer foci were anteriorly located beyond the conventional area sampled by posterior biopsies. One-fifth of cancer foci were within 6 mm of the apex. Limitations include that cystoprostatectomy cancer foci are biologically at an earlier stage than screening-detected cancers. These results created the rationale for hypothesizing that AFMS cancers originate from anterior and medial TZ but become excluded from the TZ, anteriorly into the AFMS, due to growth of BPH. The TZ anterior limit would then function as a barrier to their posterior extension.

In summary, PZ (foci <2 cc), TZ/AFMS cancer contours and locations can be predictable and conform to histological zonal boundaries.

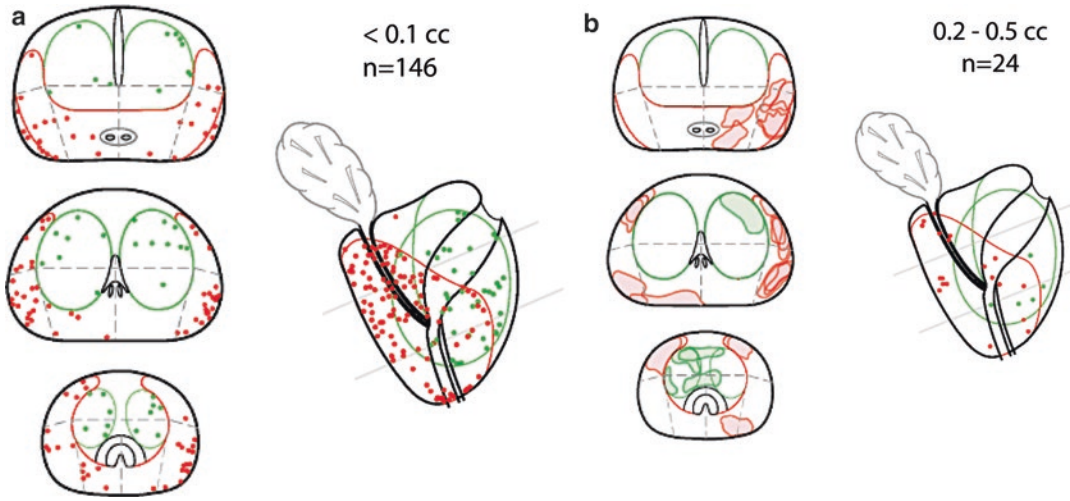

Fig. 7.4 Spatial distribution of (**a**) 146 prostate cancers <0.1 cc and (**b**) 24 prostate cancers 0.2–0.5 cc on sagittal and transverse prostate sections for an average 45 cc gland. *Dots* represent the center of each cancer focus. PZ cancers are in *red* and TZ/AFMS in *green*. Modified with permission from Nevoux P, Ouzzane A, Ahmed HU, Emberton M, Montironi R, Presti JC, Jr., et al. Quantitative tissue analyses of prostate cancer foci in an unselected cystoprostatectomy series. BJU Int. 2012 Aug;110(4):517–523 [60]

Knowledge of cancer origin and intraprostatic pattern of dissemination can be important for imaging, diagnosis, and guidance for biopsy and focal therapy. Additional study will be necessary to better understand the molecular events and potential intraprostatic spread of cancers within the prostate.

Accuracy of Novel Imaging-Guided Biopsies Validated by Final Pathology Assessment of Prostatectomy Specimens

To date, there is a lack of specific and sensitive imaging to accurately identify the extent or contours of significant cancer foci. In a milestone paper, Siddiqui et al. presented extensive experience from the National Cancer Institute (NCI) with fusion MRI/TRUS-guided biopsy [61]. Within the group of 170 who underwent prostatectomy, 17 patients were diagnosed only on standard biopsy, of whom 3 (18 %) had intermediate- or high-risk cancer on whole-mount pathology. By contrast, 20 patients were diagnosed with prostate cancer only on targeted biopsy, of whom 12 (60 %) had intermediate- or high-risk cancer on whole-mount pathology. When the ability of preoperative biopsy to predict whole-gland pathology was examined, the sensitivity of targeted biopsy was 77 % vs. 53 % for standard biopsy, while the specificities were similar (targeted, 68 %, vs. standard, 66 %). The area under the receiver operating curve (AUC) for targeted biopsy (0.73) was significantly greater than that of either standard biopsy (0.59, $P = 0.005$) or combined biopsy (0.67, $P = 0.04$) [61].

At the NCI, Turkbey et al. developed the customized mold and provided tissue blocks that permitted a direct one-to-one correlation with in vivo MRI [62, 63]. The use of the customized mold enabled more exact correlation between each MRI parameter and the histopathological specimen, without requiring a correction or an approximation approach to validate MRI with a more standardized, unbiased method. Whole-mount histopathological evaluation of 45 prostatectomy specimens revealed 342 tumor-positive regions: 281 (82 %) in the PZ and 61 (18 %) in the central zone (CZ) among 1746 regions. Of these 342 tumor positive regions, 90 (82 %) in the PZ and 20 (18 %) in the CZ contained tumors 5 mm or less in diameter, whereas 232 including 191 (82 %) in the PZ and 41 (18 %) in the CZ

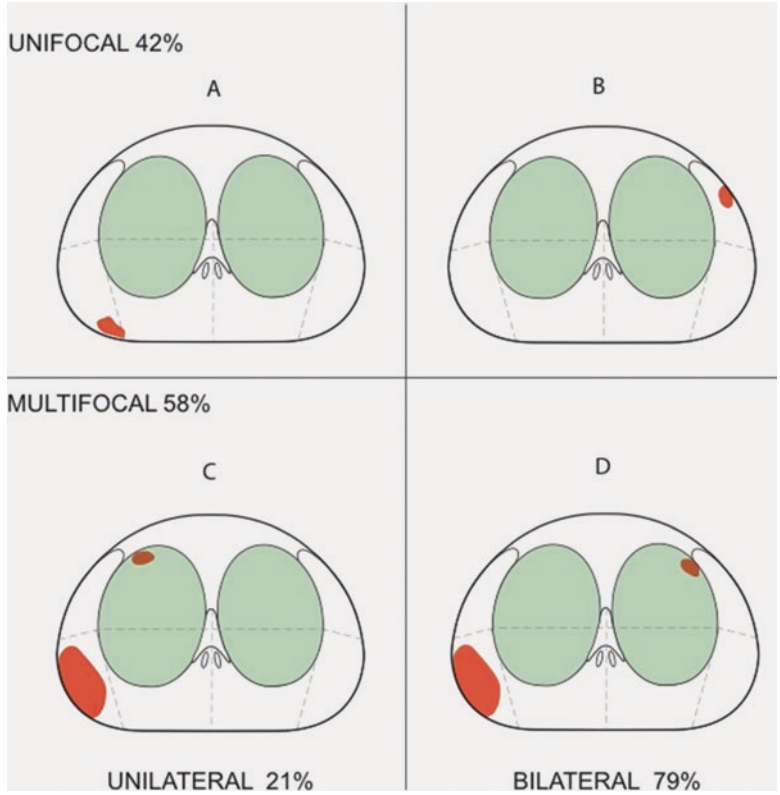

Fig. 7.5 Average transverse section of a 45 cc prostate at mid-gland depicting a model of distribution of 215 separate prostate cancers in 96 cystoprostatectomy specimens demonstrating unifocal (**a**, **b**) and multifocal (**c**, **d**), unilateral (**c**), and bilateral (**d**) tumors. Among the unilateral and multifocal cases (**c**), cancers were in the same anterior or posterior part of the gland in 50 % of cases. (**a**) Posterior insignificant cancer of 0.1 cc that could be detected by posterior systematic biopsies (SB). (**b**) Anterior insignificant cancer of 0.1 cc undetectable by posterior SB. (**c**, **d**) Unilateral (**c**) and bilateral (**d**) multifocal cancers with a large PZ cancer of 0.7 cc and a smaller TZ cancer of 0.1 cc. Modified with permission from Nevoux P, Ouzzane A, Ahmed HU, Emberton M, Montironi R, Presti JC, Jr., et al. Quantitative tissue analyses of prostate cancer foci in an unselected cystoprostatectomy series. BJU Int. 2012 Aug;110(4):517–523 [60]

contained tumors greater than 5 mm in diameter. Gleason scores were 7 or less in 235 regions: 194 (82.5 %) in the PZ and 41 (17.5 %) in the CZ regions and greater than 7 in 107 regions; 87 (81 %) in the PZ and 20 (19 %) in the CZ regions. On histopathological evaluation, extracapsular extension was detected in 20 regions in 12 prostatectomy specimens. Seminal vesicle invasion was detected in two patients. The positive predictive value of mpMRI to detect prostate cancer was 98 %, 98 %, and 100 % in the overall prostate, peripheral zone, and central gland, respectively. The sensitivity of MRI sequences was higher for tumors larger than 5 mm in diameter as well as for those with higher Gleason scores (greater than 7, $p < 0.05$) [63].

In prior studies to correct the mismatches between MRI and histopathology, several methods have been proposed. Scheidler et al. considered tumor sites detected on MRI and histopathology if they were in the same sextant within a range of 1 section (±3 to 4 mm craniocaudally) provided that they were in the same anterior or posterior prostatic hemisphere [64]. Villers et al. matched MRI with histopathology based on anatomical landmarks such as gland contours [65]. Other groups accepted a distance of 8 mm to 10 mm (approximately 2 sections) as evidence of a match between MRI and histopathology [66, 67].

Russo et al. presented results of 115 patients with biopsy-confirmed prostate cancer who

underwent mpMRI before radical prostatectomy [68]. Stained whole-mount histological sections were used as the reference standard. All lesions were contoured by an experienced uropathologist who assessed their volume and pathological Gleason score. All lesions with a volume of >0.5 ml and/or pathological Gleason score of > 6 were defined as clinically significant prostate cancer. In all, 104 of 115 index lesions were correctly diagnosed by mpMRI with sensitivity—90.4 % and 95 % confidence interval (CI) 83.5–95.1 %, including 98/105 clinically significant index lesions (93.3 %; 95 % CI 86.8–97.3 %), among which 3 of 3 lesions had a volume of <0.5 ml and Gleason score of >6. Overall, mpMRI detected 131/206 lesions, including 13 of 68 "insignificant" prostate cancers (Table 7.2) [68]. The multivariate logistic regression modeling showed that pathological Gleason score (odds ratio [OR] 11.7, 95 % CI 2.3–59.8; $P = 0.003$) and lesion volume (OR 4.24, 95 % CI 1.3–14.7; $P = 0.022$) were independently associated with the detection of index lesions at MRI.

In conclusion, fusion MRI/TRUS-targeted biopsy:

- Improves the cancer detection rate, especially Gleason score high-grade ≥7 tumors, but does not replace systematic biopsy making it complimentary.
- Undergrades 20–30 % of tumors particularly those with tertiary pattern grade.
- Misses (false-negative result) up to 30 % of clinically significant cancer lesions.
- Overall, mpMRI detects 80 % of index and 50 % of all prostate cancers.
- Significantly underestimates tumor diameter and volume for apex-base (longitudinal) dimension more than anterior-posterior and left-right (axial) dimension with large standard deviation that cannot predict in individual cases an actual tumor location.
- To date, results of fusion biopsy with spatial distribution of PCa are not reliable to plan a focal targeted therapy in case of switching patients from AS toward interventional therapy.

Ultimately, we believe that the 3DBiopsy™ System (3DBiopsy, Inc.) can potentially overcome the limitations of fusion biopsy.

There are several studies in the literature comparing the accuracy of transrectal and transperineal biopsy with computer simulation on reconstructed 3D computer models of radical whole-mount specimens [69]. Hu et al. determined the effectiveness of two sampling strategies: repeat TRUS biopsy and transperineal template-guided mapping biopsy (TTMB) to detect and exclude lesions of ≥0.2 ml or ≥0.5 ml [70].

Table 7.2 Per-index lesion sensitivity of mp-MRI according to pathological Gleason score and location

Sensitivity, % (*n/N*)					
	Gleason score ≤6	Gleason score 3+4	Gleason score 4+3	Gleason score ≥8	Total
All lesions					
PZ	28.1 (18/64)	85.1 (63/74)	100 (22/22)	93.7 (15/16)	67 (118/176)
TZ	30 (6/20)	71.4 (5/7)	50 (1/2)	100 (1/1)	43.3 (13/30)
Total	28.6 (24/84)	83.9 (68/81)	95.8 (23/24)	94.1 (16/17)	63.6 (131/206)
Clinically significant lesions (>0.5 ml or ≤0.5 ml and Gleason score ≥7)					
PZ	70 (7/10)	85.1 (63/74)	100 (22/22)	93.7 (15/16)	87.7 (107/122)
TZ	66.6 (4/6)	71.4 (5/7)	50 (1/2)	100 (1/1)	68.8 (11/16)
Total	68.7 (11/16)	83.9 (68/81)	95.8 (23/24)	94.1 (16/17)	85.5 (118/138)

Data are percentages, numerators indicate the number of detected lesions, and denominators represent the total number of lesions

PZ peripheral zone, *TZ* transitional zone

Reprinted with permission from Russo F, Regge D, Armando E, Giannini V, Vignati A, Mazzetti S, et al. Detection of prostate cancer index lesions with multiparametric magnetic resonance imaging (mp-mri) using whole-mount histological sections as the reference standard. BJU Int. 2016 Jul;118(1):84–94 [68]

In 107 consecutive cases that were analyzed with TTMB and five different TRUS biopsy strategies that were simulated, the latter involved a standard 12-core sampling and incorporated variable amounts of error, as well as the addition of anterior cores ≥0.5 ml. Overall, TTMB accuracy (AUC) was ≈0.90 compared with AUC 0.70–0.80 for TRUS biopsy. In addition, at best, TRUS biopsy missed 30–40 % of lesions of ≥0.2 ml and ≥0.5 ml, while TTMB missed 5 % of such lesions.

Muthuveloe et al. conducted a prospective study of 200 consecutive men who underwent template biopsy in a tertiary referral center, using a standard 24-region template prostate biopsy technique [71]. Overall detection rate was 47 %; 39.5 % of cases with previous negative transrectal biopsies were found to have prostate adenocarcinoma; and 47.5 % of cases on AS for Gleason 3+3 = 6 prostate adenocarcinoma were upgraded. The authors concluded that those considering AS for Gleason 3+3 = 6 disease should be offered template biopsy to confirm the grade of their disease.

Ayres et al. evaluated the role of TTMB in 101 men on active surveillance at a single center [72]. Criteria for active surveillance were ≤75 years, Gleason ≤3+3, PSA ≤ 15 ng/ml, clinical stage T1–2a, and ≤50 % TRUS guided transrectal biopsy cores positive for cancer with ≤10 mm of disease in a single core. The number of men with an increase in disease volume or Gleason grade on TTMB and the number of men who later underwent radical treatment were assessed. In all, 34 % of men had more significant prostate cancer on restaging transperineal template biopsies compared with their transrectal biopsies. Of these men, 44 % had disease predominantly in the anterior part of the gland, an area often undersampled by transrectal biopsies. In the group of men who had restaging TTMB within 6 months of commencing active surveillance, 38 % had more significant disease. In total, 33 % of men stopped active surveillance and had radical treatment. In conclusion, around one-third of men had more significant prostate cancer on TTMB. This probably reflects under-sampling by initial transrectal biopsies rather than disease progression.

Crawford et al. correlated the clinical-pathologic results of 1403 TTMB cores obtained from 25 men diagnosed with PCa with 64 cancer lesions found in their corresponding RP specimens [73]. Special computer models of 3D whole-mounted radical prostatectomy (3D–WMRP) specimens were generated and used as a gold standard to determine tumor morphometric data. Between-sample rates of upgrade and downgrade (highest GS and a novel cumulative GS) and upstage and downstage (laterality) were determined. Lesions ≥0.5 cm^3 or GS ≥ 7 were considered clinically significant. From 64 separate 3D–WMRP lesions, 25 had significant volume (mean 1.13 cm^3) and 39 were insignificant (mean 0.09 cm^3) ($P < 0.0001$); 18/64 lesions were missed by TTMB, but only 1 was clinically significant with GS-8 (0.02 cm^3). When comparing the cumulative GS of TTMB versus RP, 72 % ($n = 18$) had identical scores, 12 % ($n = 3$) were upgraded, and only 16 % ($n = 4$) were downgraded. Laterality of TTMB and RP was strongly correlated, 80 % same laterality, 4 % were upstaged, and 16 % downstaged. Finally, they demonstrated that TTMB using a 5 mm sampling frame had 95 % sensitivity and 30 % specificity to detect 0.5 ml lesions.

A number of clinical studies have shown that TTMB detects more cancer, identifies bilateral disease in men thought to have unilateral cancer, upgrades disease in approximately a third of patients, and provides localization information on individual lesions [72, 74, 75]. As a result, TTMB could be used to select men for active surveillance or focal therapy. This may decrease the 30–40 % delayed intervention rate currently seen in active surveillance cohorts and decrease the need for intensive biopsy surveillance.

The technique of TTMB is evolving to improve the outcomes of its diagnostic accuracy. Barzell and Melamed assessed 80 patients, in whom focal cryoablation was planned, with both TTMB and TRUS biopsy [76]. In their study, 47 % of patients found suitable by TRUS biopsy for focal therapy actually had high-risk cancer in TTMB. However, the technique used in that study is different from the present definition for mapping biopsy, and, according to the Ginsburg Study Group, Barzell's technique might be

termed as "transperineal template-guided saturation biopsy." Onik and Barzell used the Crawford model of TTMB to carry out mapping biopsy in 110 patients with TRUS biopsy-proven unilateral disease. They showed that TTMB found bilateral disease in 55 % and Gleason upgrading in 25 % of patients.

Sivaraman et al. carried out volume-based TTMB in 98 patients with low-risk PCa diagnosed by TRUS biopsy and found that 30.6 % of the patients were upstaged/upgraded (9.2 % had bilateral disease, 16.3 % had Gleason upgrade, and 5.1 % had both) [77]. According to present evidence, the cancer detection rate of TTMB after initial negative TRUS biopsy is 46–68 %. Diagnostic performance of TTMB in the initial biopsy setting is 73–76 %, which is superior to all the diagnostic modalities used for PCa to date. These data reflect the superior results of TTMB in detecting, grading, and mapping of PCa as compared with TRUS biopsy.

The results of TTMB are very encouraging, and it will potentially become an essential tool for the management of PCa. Future studies will broaden the indications of this excellent technique and define the limitations. Considering the exceptional cancer detection rate of TTMB, its use in the primary biopsy setting remains to be seen. However, the cost-benefit ratio of the procedure in this setting will determine the utility. Advances in image-guided mpMRI biopsies have enhanced TRUS biopsy cancer detection. Prebiopsy imaging or real-time image guidance can guide the clinician to cluster more high-quality cores with longer core distance covering a whole length. The differential clustering of cores within the prostate depending on image guidance could culminate in a superior cancer detection rate with exact spatial distribution of prostate cancer. Fusion of imaging with grid sampling will be an interesting advance in PCa diagnosis and can form the basis for future research in prostate biopsy techniques.

The definition of insignificant cancer for TTMB must be revisited and redefined. These attributes can potentially overcome most of the shortcomings of the present biopsy techniques. Huo et al., in their retrospective diagnostic accuracy study, compared the results of primary transperineal biopsies with the radical prostatectomy pathology of 414 consecutive patients treated at a single institution [78]. The average sensitivity and specificity for the detection of cancer in all prostates across all biopsy zones was 48 % (95 % CI 42.6–53.4) and 84.1 % (95 % CI 80–88.2), respectively. Interestingly, there was a statistically significant decrease in the sensitivity of transperineal biopsy in larger prostates. Grading concordance between biopsy and pathology specimens was achieved in 65.7 % of patients. Upgrading of Gleason scores occurred in 25.6 % of patients and downgrading occurred in 8.8 %. Thus, their transperineal biopsy method has demonstrated fair agreement with the histopathology findings of the corresponding radical prostatectomy specimens. The cancer detection rate was lower in larger prostates, suggesting an increase in the number of cores in larger prostates as a strategy to improve cancer detection.

A few randomized studies demonstrated that combined biopsy approach (fusion MRI/TRUS-targeted biopsy and transperineal multicore mapping biopsy) detects more significant PCa than fusion MRI/TRUS-targeted biopsy alone; however, it will double the detection rate of insignificant PCa [69]. For instance, Ting et al. performed a head-to-head comparison of 48 patients who underwent MRI/TRUS-targeted biopsy (TBx) and 80 patients underwent combined MRI/TRUS-targeted biopsy plus 24-core saturation TTMB [79]. In the MRI/TRUS-targeted biopsy versus combined biopsy strategy subgroup analysis ($n = 80$), there were 55 PCa and 38 significant PCa. The detection rate for the combined biopsy strategy versus MRI/TRUS-TBx for significant PCa was 49 % versus 40 % ($p = 0.02$) and for insignificant PCa was 20 % versus 10 % ($p = 0.04$), respectively. Eleven cases (14 %) of significant PCa were detected exclusively on MRI/TRUS-TBx and 7 cases (8.7 %) of significant PCa were detected exclusively on TTMB.

Radtke et al. reported a comparative analysis of 294 consecutive patients undergoing systematic transperineal biopsy and MRI/TRUS fusion TBx [80]. The authors reported that sampling efficiency was in favor of the second method,

with 46.0 % of MRI/TRUS fusion TB vs. 7.5 % of systematic biopsy cores detecting PCa with a Gleason score >7. However, there was still utility to perform systematic transperineal sampling, as 12.8 % Gleason score >7 were missed by the targeted approach. The opposite occurred in 20.9 %. The authors concluded that the gold standard for cancer detection is a combination of systematic and targeted cores.

In a recent review of the literature, Toner et al. demonstrated that mpMRI has an increasing role for PCa diagnosis, staging, and directing management toward improving patient outcomes [81]. Compared with radical prostatectomy RP and TTMB specimens, the sensitivity and specificity of mpMRI reported in the literature are approximately 80–90 % and 50–90 % (Table 7.3 [82–88] and Table 7.4 [82, 89–92]).

The Safety Margin of Focal Ablation Based on Concordance Between Baseline Multiparametric Magnetic Resonance Imaging and Final Pathology Assessment

Ideally, FT will completely treat all histologic malignancy, not just what is visible on imaging. At University of California, Los Angeles (UCLA), Priester et al. demonstrated that MRI consistently underestimates the size and extent of prostate tumors [93]. The study examined 114 men who had mpMRI before radical prostatectomy with patient-specific mold processing of the specimen. T2-weighted images were used to contour the prostate capsule and cancer-suspicious regions of interest (ROIs). The contours were used to design and 3D-print custom molds, which permitted alignment of excised prostates with MR images. Tumors were reconstructed in 3D from digitized whole-mount sections. Tumors were then matched with ROIs and their relative geometries were compared. At final pathology assessment, 222 tumors were evident on whole-mount sections, 118 of which had been identified on MRI. For the 118 ROIs, the mean volume was 0.8 cc and the longest 3D diameter was 17 mm. However, for matched pathologic tumors, most of which were GS ≥3+4, the mean volume was 2.5 cc and the longest 3D diameter was 28 mm. The median tumor had a 13.5 mm maximal extent beyond the MRI contour, and 80 % of cancer volume from matched tumors was outside of ROI boundaries. Size estimation was most accurate in the axial plane and least accurate along the base-apex axis. Prostate cancer foci had an average diameter 11 mm longer and a volume 3 times greater than T2-weighted MRI segmentations. These results may have important implications for improving accuracy, especially along the base-apex axis.

Table 7.3 Comparison data of multiparametric magnetic resonance imaging (mpMRI) with radical prostatectomy as a reference standard

Reference	*N*	Sensitivity (%)	Specificity (%)	NPV	PPV	Definition of significant PCa
Thompson et al. [82]	48	98	43	75	91	GS ≥ 7, GS = 6 CL ≥ 5 mm or 20 % cores positive
Chamie et al. [83]	115	96	46	92	66	pT3, GS ≥ 4+3, GS = 3+4 and ≥1.3 ml
Junker et al. [84]	50	97	79	NR	NR	Any PCa
Hoeks et al. [85]	63	65	67	NR	NR	Any PCa
Delongchamps et al. [86]	57	78	97	NR	NR	Any PCa
Yoschizako et al. [87]	35	69	94	NR	95	Any PCa
Villers et al. [88]	24	77	91	NR	NR	Any PCa

N number of radical prostatectomies, *NPV* negative predictive value, *PPV* positive predictive value, *PCa* prostate cancer, *GS* Gleason score, *CL* core length

Table 7.4 Comparison of multiparametric magnetic resonance imaging (mpMRI) with transperineal mapping biopsy (TPMB) as a reference control

Reference	*N*	Sensitivity (%)	Specificity (%)	NPV	PPV	Definition of significant PCa	Number of cores	Reporting system
Pepe et al. [89]	168	83	72	88	79	NR	6–35, median 28	NR
Thompson et al. [82]	150	93	53	52	98	GS ≥ 7, GS = 6 CL ≥ 5 mm or 20 % cores positive	median 30, two targeted	PI-RADS
Grey et al. [90]	201	97	60	98	49, 58, 84[a]	GS ≥ 7, GS = 6 CL ≥ 6 mm	24–40, two to four targeted	PI-RADS
Abd- Alazeez et al. [91]	54	90, 76	42, 42	95, 79	26, 38	UCL 1, UCL 2[b]	Minimum 10–12	PI-RADS
Arumainayagam et al. [92]	64	64–81, 58–73[c]	68–80, 71–83[c]	91–94, 84–89[c]	35–45, 49–63[c]	UCL 1, UCL 2[b]	29–41, median 34	Likert

N number of patients, *NPV* negative predictive value, *PPV* positive predictive value, *PCa* prostate cancer, *GS* Gleason score, *CL* core length, *PI-RADS* Prostate Imaging Reporting and Data System, *UCL* University College London

[a]PPV for PI-RADS 3, 4, and 5, respectively

[b]UCL 1, Gleason score of over 4+3 and/or maximum cancer core length (CCL_{max}) of 6 mm or more; UCL 2, Gleason score of 3+4 or more and/or CCL_{max} of 4 mm or more

[c]Range from different radiologists

The latest report of this group updated results showing an index PCa detection rate by mpMRI in 224 of 285 (78.6 %) tumors validated by whole-mount histopathology (WMHP) (Carroll P. Personal communication, 2016). The median maximal diameter of PCa index tumors on mpMRI was 1.3 cm while on WMHP measured as 2.0 cm with poor Pearson correlation coefficient of 0.45 ($p < 0.05$).

Le Nobin et al. examined the accuracy of 3 Tesla MRI before prostatectomy in 33 patients [11]. Concordance was conducted between lesion borders traced by a radiologist on MRI images and MRI and 3D reconstructions created from high-resolution digitalized slides of radical prostatectomy specimens and co-registered to imaging using advanced software. Tumors were compared between histology and imaging by the Hausdorff distance and stratified by the MRI suspicion score, Gleason score, and lesion diameter. The results showed a boundary underestimation in larger lesions with an imaging suspicion score 4 or greater (mean 3.49 ± 2.1 mm, $p < 0.001$) and a Gleason score of 7 or greater (mean 2.48 ± 2.8 mm, $p = 0.035$). A simulated treatment volume based on the MRI boundary missed an average 14.8 % of tumor volume compared to that based on the histological boundary (Fig. 7.6) [11]. Adjustment of simulated treatment volume to a 9 mm treatment margin achieved complete

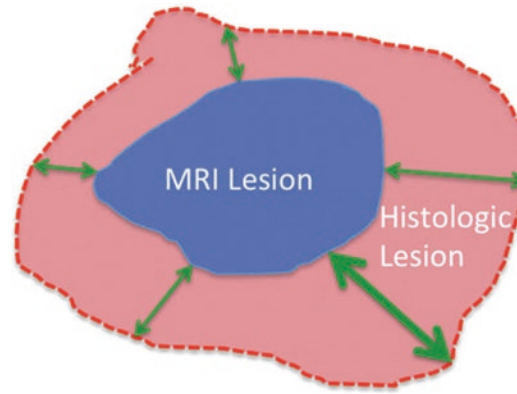

Fig. 7.6 Cartoon reconstruction of MRI-visible lesion (*blue boundary*) within actual histologic lesion (*pink boundary*). Note that the MRI-visible lesion underestimates the true histologic lesion. The *large two-headed arrow* indicates the maximum Hausdorff distance from the center of the lesion. Reprinted with permission from Le Nobin J, Rosenkrantz AB, Villers A, Orczyk C, Deng FM, Melamed J, et al. Image guided focal therapy for magnetic resonance imaging visible prostate cancer: Defining a 3-dimensional treatment margin based on magnetic resonance imaging histology co-registration analysis. J Urol. 2015 Aug;194(2):364–370 [11]

histological tumor destruction in 100 % of patients and should be incorporated into clinical ablation strategies.

Conclusion

The fast-growing implementation of organ-sparing approaches such as AS and FT has gained popularity in today's clinical practice both by patients and physicians alike due to the desire to avoid overtreatment and minimize the potential side effects of incontinence and impotence often associated with whole-gland therapy. The early detection of PCa with the introduction of advanced pathologic and genomics techniques has resulted in more frequent diagnoses of small tumors of lower volume and clinical stage that can be unifocal and/or unilateral, thus supporting the concept of AS and parenchyma-sparing FT. The several novel studies based on unbiased genome-wide approaches coupled with pathologic assessment demonstrated that anatomically distinct tumor metastases are derived from a single progenitor clone. These data of the literature suggest that most commonly the driver lesion with potentially lethal clone is located inside of index focus that gives the bright prospects for focal ablation of this focus with potentially curable intent. However, currently, we still lack a reliable diagnostic tool to rule out an existence of this lethal clone in secondary (satellite) lesion(s) in some cohort of patients.

References

1. Klotz L, Emberton M. Management of low risk prostate cancer: active surveillance and focal therapy. Curr Opin Urol. 2014;24(3):270–9.
2. Polascik TJ, Passoni NM, Villers A, Choyke PL. Modernizing the diagnostic and decision-making pathway for prostate cancer. Clin Cancer Res. 2014;20(24):6254–7.
3. van der Poel H, Klotz L, Andriole G, Azzouzi AR, Bjartell A, Cussenot O, et al. Role of active surveillance and focal therapy in low- and intermediate-risk prostate cancers. World J Urol. 2015;33(7):907–16.
4. Mouraviev V, Villers A, Bostwick DG, Wheeler TM, Montironi R, Polascik TJ. Understanding the pathological features of focality, grade and tumour volume of early-stage prostate cancer as a foundation for parenchyma-sparing prostate cancer therapies: active surveillance and focal targeted therapy. BJU Int. 2011;108(7):1074–85.
5. Muir G. Focal prostate therapy: will we ever know the best energy? BJU Int. 2014;113(1):8.
6. Polascik TJ, Mouraviev V. Focal therapy for prostate cancer is a reasonable treatment option in properly selected patients. Urology. 2009;74(4):726–30.
7. Sartor AO, Hricak H, Wheeler TM, Coleman J, Penson DF, Carroll PR, et al. Evaluating localized prostate cancer and identifying candidates for focal therapy. Urology. 2008;72(6 Suppl):S12–24.
8. Schmidt C. Focal therapy gains ground in low-risk prostate cancer. J Natl Cancer Inst. 2015;107(9).
9. Polascik TJ. Focal therapy of prostate cancer: making steady progress toward a first-line image-guided treatment modality. Curr Opin Urol. 2015;25(3):183–4.
10. Mendez MH, Joh DY, Gupta R, Polascik TJ. Current trends and new frontiers in focal therapy for localized prostate cancer. Curr Urol Rep. 2015;16(6):35.
11. Le Nobin J, Rosenkrantz AB, Villers A, Orczyk C, Deng FM, Melamed J, et al. Image guided focal therapy for magnetic resonance imaging visible prostate cancer: defining a 3-dimensional treatment margin based on magnetic resonance imaging histology co-registration analysis. J Urol. 2015;194(2):364–70.
12. Haffner MC, De Marzo AM, Yegnasubramanian S, Epstein JI, Carter HB. Diagnostic challenges of clonal heterogeneity in prostate cancer. J Clin Oncol. 2015;33(7):e38–40.
13. Liu W, Laitinen S, Khan S, Vihinen M, Kowalski J, Yu G, et al. Copy number analysis indicates monoclonal origin of lethal metastatic prostate cancer. Nat Med. 2009;15(5):559–65.
14. Mehra R, Tomlins SA, Yu J, Cao X, Wang L, Menon A, et al. Characterization of tmprss2-ets gene aberrations in androgen-independent metastatic prostate cancer. Cancer Res. 2008;68(10):3584–90.
15. Aryee MJ, Liu W, Engelmann JC, Nuhn P, Gurel M, Haffner MC, et al. DNA methylation alterations exhibit intraindividual stability and interindividual heterogeneity in prostate cancer metastases. Sci Transl Med. 2013;5(169):169ra110.
16. Postema AW, De Reijke TM, Ukimura O, Van den Bos W, Azzouzi AR, Barret E, et al. Standardization of definitions in focal therapy of prostate cancer: report from a delphi consensus project. World J Urol. 2016;34(10):1373–82.
17. Valerio M, Ahmed HU, Emberton M, Lawrentschuk N, Lazzeri M, Montironi R, et al. The role of focal therapy in the management of localised prostate cancer: a systematic review. Eur Urol. 2014;66(4):732–51.
18. Valerio M, Emberton M, Ahmed HU. Focal therapy will become a standard option for selected men with localized prostate cancer. J Clin Oncol. 2014;32(32):3680–1.
19. Eggener S, Salomon G, Scardino PT, De la Rosette J, Polascik TJ, Brewster S. Focal therapy for prostate

cancer: possibilities and limitations. Eur Urol. 2010;58(1):57–64.
20. Emberton M. Why focal therapy is a legitimate and necessary response to a changing world. J Urol. 2015;194(4):875–6.
21. Villers A, McNeal JE, Freiha FS, Stamey TA. Multiple cancers in the prostate. Morphologic features of clinically recognized versus incidental tumors. Cancer. 1992;70(9):2313–8.
22. Wolters T, Montironi R, Mazzucchelli R, Scarpelli M, Roobol MJ, van den Bergh RC, et al. Comparison of incidentally detected prostate cancer with screen-detected prostate cancer treated by prostatectomy. Prostate. 2012;72(1):108–15.
23. Masterson TA, Cheng L, Koch MO. Pathological characterization of unifocal prostate cancers in whole-mount radical prostatectomy specimens. BJU Int. 2011;107(10):1587–91.
24. Mouraviev V, Madden JF. Focal therapy for prostate cancer: pathologic basis. Curr Opin Urol. 2009;19(2):161–7.
25. Mouraviev V, Mayes JM, Polascik TJ. Pathologic basis of focal therapy for early-stage prostate cancer. Nat Rev Urol. 2009;6(4):205–15.
26. Karavitakis M, Ahmed HU, Abel PD, Hazell S, Winkler MH. Tumor focality in prostate cancer: implications for focal therapy. Nat Rev Clin Oncol. 2011;8(1):48–55.
27. Karavitakis M, Winkler M, Abel P, Livni N, Beckley I, Ahmed HU. Histological characteristics of the index lesion in whole-mount radical prostatectomy specimens: implications for focal therapy. Prostate Cancer Prostatic Dis. 2011;14(1):46–52.
28. Huang CC, Deng FM, Kong MX, Ren Q, Melamed J, Zhou M. Re-evaluating the concept of "dominant/index tumor nodule" in multifocal prostate cancer. Virchows Arch. 2014;464(5):589–94.
29. Mizuno R, Nakashima J, Mukai M, Ookita H, Nakagawa K, Oya M, et al. Maximum tumor diameter is a simple and valuable index associated with the local extent of disease in clinically localized prostate cancer. Int J Urol. 2006;13(7):951–5.
30. Ding Z, Wu CJ, Chu GC, Xiao Y, Ho D, Zhang J, et al. Smad4-dependent barrier constrains prostate cancer growth and metastatic progression. Nature. 2011;470(7333):269–73.
31. Ahmed HU. The index lesion and the origin of prostate cancer. N Engl J Med. 2009;361(17):1704–6.
32. Noguchi M, Stamey TA, McNeal JE, Nolley R. Prognostic factors for multifocal prostate cancer in radical prostatectomy specimens: lack of significance of secondary cancers. J Urol. 2003;170(2 Pt 1):459–63.
33. Haffner J, Potiron E, Bouye S, Puech P, Leroy X, Lemaitre L, et al. Peripheral zone prostate cancers: location and intraprostatic patterns of spread at histopathology. Prostate. 2009;69(3):276–82.
34. Algaba F, Montironi R. Impact of prostate cancer multifocality on its biology and treatment. J Endourol. 2010;24(5):799–804.
35. Arora R, Koch MO, Eble JN, Ulbright TM, Li L, Cheng L. Heterogeneity of gleason grade in multifocal adenocarcinoma of the prostate. Cancer. 2004;100(11):2362–6.
36. Andreoiu M, Cheng L. Multifocal prostate cancer: biologic, prognostic, and therapeutic implications. Hum Pathol. 2010;41(6):781–93.
37. Mai KT, Roustan Delatour NL, Assiri A, Al-Maghrabi H. Secondary prostatic adenocarcinoma: a cytopathological study of 50 cases. Diagn Cytopathol. 2007;35(2):91–5.
38. Barbieri CE, Demichelis F, Rubin MA. The lethal clone in prostate cancer: Redefining the index. Eur Urol. 2014;66(3):395–7.
39. Haffner MC, Mosbruger T, Esopi DM, Fedor H, Heaphy CM, Walker DA, et al. Tracking the clonal origin of lethal prostate cancer. J Clin Invest. 2013;123(11):4918–22.
40. Kumar A, White TA, MacKenzie AP, Clegg N, Lee C, Dumpit RF, et al. Exome sequencing identifies a spectrum of mutation frequencies in advanced and lethal prostate cancers. Proc Natl Acad Sci U S A. 2011;108(41):17087–92.
41. Grasso CS, Wu YM, Robinson DR, Cao X, Dhanasekaran SM, Khan AP, et al. The mutational landscape of lethal castration-resistant prostate cancer. Nature. 2012;487(7406):239–43.
42. Barbieri CE, Baca SC, Lawrence MS, Demichelis F, Blattner M, Theurillat JP, et al. Exome sequencing identifies recurrent spop, foxa1 and med12 mutations in prostate cancer. Nat Genet. 2012;44(6):685–9.
43. Fraser M, Berlin A, Bristow RG, van der Kwast T. Genomic, pathological, and clinical heterogeneity as drivers of personalized medicine in prostate cancer. Urol Oncol. 2015;33(2):85–94.
44. Bostwick DG, Shan A, Qian J, Darson M, Maihle NJ, Jenkins RB, et al. Independent origin of multiple foci of prostatic intraepithelial neoplasia: comparison with matched foci of prostate carcinoma. Cancer. 1998;83(9):1995–2002.
45. Djavan B, Susani M, Bursa B, Basharkhah A, Simak R, Marberger M. Predictability and significance of multifocal prostate cancer in the radical prostatectomy specimen. Tech Urol. 1999;5(3):139–42.
46. Ohori M, Kattan M, Scardino PT, Wheeler TM. Radical prostatectomy for carcinoma of the prostate. Mod Pathol. 2004;17(3):349–59.
47. Branca RT, Chen YM, Mouraviev V, Galiana G, Jenista ER, Kumar C, et al. Idqc anisotropy map imaging for tumor tissue characterization in vivo. Magn Reson Med. 2009;61(4):937–43.
48. Mouraviev V, Mayes JM, Sun L, Madden JF, Moul JW, Polascik TJ. Prostate cancer laterality as a rationale of focal ablative therapy for the treatment of clinically localized prostate cancer. Cancer. 2007;110(4):906–10.
49. Yoon GS, Wang W, Osunkoya AO, Lane Z, Partin AW, Epstein JI. Residual tumor potentially left behind after local ablation therapy in prostate adenocarcinoma. J Urol. 2008;179(6):2203–6. discussion 2206

50. Bott SR, Ahmed HU, Hindley RG, Abdul-Rahman A, Freeman A, Emberton M. The index lesion and focal therapy: an analysis of the pathological characteristics of prostate cancer. BJU Int. 2010;106(11):1607–11.
51. Ahmed HU, Freeman A, Kirkham A, Sahu M, Scott R, Allen C, et al. Focal therapy for localized prostate cancer: a phase I/II trial. J Urol. 2011;185(4):1246–54.
52. Epstein JI, Egevad L, Humphrey PA, Montironi R. Members of the IIiDUPG. Best practices recommendations in the application of immunohistochemistry in the prostate: report from the international society of urologic pathology consensus conference. Am J Surg Pathol. 2014;38(8):e6–e19.
53. Van der Kwast T. Gleason score 7: when qualitative change becomes quantitative change. J Urol. 2016;196(2):303–4.
54. Tollefson MK, Leibovich BC, Slezak JM, Zincke H, Blute ML. Long-term prognostic significance of primary Gleason pattern in patients with Gleason score 7 prostate cancer: impact on prostate cancer specific survival. J Urol. 2006;175(2):547–51.
55. Burdick MJ, Reddy CA, Ulchaker J, Angermeier K, Altman A, Chehade N, et al. Comparison of biochemical relapse-free survival between primary Gleason score 3 and primary Gleason score 4 for biopsy Gleason score 7 prostate cancer. Int J Radiat Oncol Biol Phys. 2009;73(5):1439–45.
56. Stark JR, Perner S, Stampfer MJ, Sinnott JA, Finn S, Eisenstein AS, et al. Gleason score and lethal prostate cancer: Does 3+4=4+3? J Clin Oncol. 2009;27(21):3459–64.
57. Ohori M, Scardino PT. Localized prostate cancer. Curr Probl Surg. 2002;39(9):833–957.
58. Weinreb JC, Barentsz JO, Choyke PL, Cornud F, Haider MA, Macura KJ, et al. PI-RADS prostate imaging – reporting and data system: 2015, version 2. Eur Urol. 2016;69(1):16–40.
59. Bouye S, Potiron E, Puech P, Leroy X, Lemaitre L, Villers A. Transition zone and anterior stromal prostate cancers: zone of origin and intraprostatic patterns of spread at histopathology. Prostate. 2009;69(1):105–13.
60. Nevoux P, Ouzzane A, Ahmed HU, Emberton M, Montironi R, Presti Jr JC, et al. Quantitative tissue analyses of prostate cancer foci in an unselected cystoprostatectomy series. BJU Int. 2012;110(4):517–23.
61. Siddiqui MM, Truong H, Rais-Bahrami S, Stamatakis L, Logan J, Walton-Diaz A, et al. Clinical implications of a multiparametric magnetic resonance imaging based nomogram applied to prostate cancer active surveillance. J Urol. 2015;193(6):1943–9.
62. Trivedi H, Turkbey B, Rastinehad AR, Benjamin CJ, Bernardo M, Pohida T, et al. Use of patient-specific MRI-based prostate mold for validation of multiparametric MRI in localization of prostate cancer. Urology. 2012;79(1):233–9.
63. Turkbey B, Mani H, Aras O, Rastinehad AR, Shah V, Bernardo M, et al. Correlation of magnetic resonance imaging tumor volume with histopathology. J Urol. 2012;188(4):1157–63.
64. Scheidler J, Weores I, Brinkschmidt C, Zeitler H, Panzer S, Scharf M, et al. Diagnosis of prostate cancer in patients with persistently elevated psa and tumor-negative biopsy in ambulatory care: performance of mr imaging in a multi-reader environment. Rofo. 2012;184(2):130–5.
65. Villers A, Lemaitre L, Haffner J, Puech P. Current status of mri for the diagnosis, staging and prognosis of prostate cancer: implications for focal therapy and active surveillance. Curr Opin Urol. 2009;19(3):274–82.
66. Eymerit-Morin C, Zidane M, Lebdai S, Triau S, Azzouzi AR, Rousselet MC. Histopathology of prostate tissue after vascular-targeted photodynamic therapy for localized prostate cancer. Virchows Arch. 2013;463(4):547–52.
67. Montironi R, Egevad L, Bjartell A, Berney DM. Role of histopathology and molecular markers in the active surveillance of prostate cancer. Acta Oncol. 2011;50(Suppl 1):56–60.
68. Russo F, Regge D, Armando E, Giannini V, Vignati A, Mazzetti S, et al. Detection of prostate cancer index lesions with multiparametric magnetic resonance imaging (MP-MRI) using whole-mount histological sections as the reference standard. BJU Int. 2016;118(1):84–94.
69. Sivaraman A, Sanchez-Salas R, Barret E, Ahallal Y, Rozet F, Galiano M, et al. Transperineal template-guided mapping biopsy of the prostate. Int J Urol. 2015;22(2):146–51.
70. Hu JC, Chang E, Natarajan S, Margolis DJ, Macairan M, Lieu P, et al. Targeted prostate biopsy in select men for active surveillance: do the Epstein criteria still apply? J Urol. 2014;192(2):385–90.
71. Muthuveloe D, Telford R, Viney R, Patel P. The detection and upgrade rates of prostate adenocarcinoma following transperineal template-guided prostate biopsy – a tertiary referral centre experience. Cent European J Urol. 2016;69(1):42–7.
72. Ayres BE, Montgomery BS, Barber NJ, Pereira N, Langley SE, Denham P, et al. The role of transperineal template prostate biopsies in restaging men with prostate cancer managed by active surveillance. BJU Int. 2012;109(8):1170–6.
73. Crawford ED, Rove KO, Barqawi AB, Maroni PD, Werahera PN, Baer CA, et al. Clinical-pathologic correlation between transperineal mapping biopsies of the prostate and three-dimensional reconstruction of prostatectomy specimens. Prostate. 2013;73(7):778–87.
74. Fernandez Gomez JM, Garcia RJ. Optimization of prostate biopsy in patients considered for active surveillance. The role of the confirmatory biopsy and transperineal techniques. Arch Esp Urol. 2014;67(5):409–18.
75. Bittner N, Merrick GS, Butler WM, Bennett A, Galbreath RW. Incidence and pathological features of prostate cancer detected on transperineal template guided mapping biopsy after negative transrectal ultrasound guided biopsy. J Urol. 2013;190(2):509–14.

76. Barzell WE, Melamed MR. Appropriate patient selection in the focal treatment of prostate cancer: the role of transperineal 3-dimensional pathologic mapping of the prostate–a 4-year experience. Urology. 2007;70(6 Suppl):27–35.
77. Sivaraman A, Sanchez-Salas R, Ahmed HU, Barret E, Cathala N, Mombet A, et al. Clinical utility of transperineal template-guided mapping biopsy of the prostate after negative magnetic resonance imaging-guided transrectal biopsy. Urol Oncol. 2015;33(7):329 e327–311.
78. Huo AS, Hossack T, Symons JL, PeBenito R, Delprado WJ, Brenner P, et al. Accuracy of primary systematic template guided transperineal biopsy of the prostate for locating prostate cancer: a comparison with radical prostatectomy specimens. J Urol. 2012;187(6):2044–9.
79. Ting F, van Leeuwen PJ, Delprado W, Haynes AM, Brenner P, Stricker PD. Tumor volume in insignificant prostate cancer: increasing the threshold is a safe approach to reduce over-treatment. Prostate. 2015;75(15):1768–73.
80. Radtke JP, Kuru TH, Boxler S, Alt CD, Popeneciu IV, Huettenbrink C, et al. Comparative analysis of transperineal template saturation prostate biopsy versus magnetic resonance imaging targeted biopsy with magnetic resonance imaging-ultrasound fusion guidance. J Urol. 2015;193(1):87–94.
81. Toner L, Weerakoon M, Bolton DM, Ryan A, Katelaris N, Lawrentschuk N. Magnetic resonance imaging for prostate cancer: comparative studies including radical prostatectomy specimens and template transperineal biopsy. Prostate Int. 2015;3(4):107–14.
82. Thompson JE, Moses D, Shnier R, Brenner P, Delprado W, Ponsky L, et al. Multiparametric magnetic resonance imaging guided diagnostic biopsy detects significant prostate cancer and could reduce unnecessary biopsies and over detection: a prospective study. J Urol. 2014;192(1):67–74.
83. Chamie K, Sonn GA, Finley DS, Tan N, Margolis DJ, Raman SS, et al. The role of magnetic resonance imaging in delineating clinically significant prostate cancer. Urology. 2014;83(2):369–75.
84. Junker D, Quentin M, Nagele U, Edlinger M, Richenberg J, Schaefer G, et al. Evaluation of the pirads scoring system for mpmri of the prostate: a whole-mount step-section analysis. World J Urol. 2015;33(7):1023–30.
85. Hoeks CM, Hambrock T, Yakar D, van de Hulsbergen-Kaa CA, Feuth T, Witjes JA, et al. Transition zone prostate cancer: detection and localization with 3-t multiparametric mr imaging. Radiology. 2013;266(1):207–17.
86. Delongchamps NB, Rouanne M, Flam T, Beuvon F, Liberatore M, Zerbib M, et al. Multiparametric magnetic resonance imaging for the detection and localization of prostate cancer: combination of t2-weighted, dynamic contrast-enhanced and diffusion-weighted imaging. BJU Int. 2011;107(9):1411–8.
87. Yoshizako T, Wada A, Uchida K, Hara S, Igawa M, Kitagaki H, et al. Apparent diffusion coefficient of line scan diffusion image in normal prostate and prostate cancer–comparison with single-shot echo planner image. Magn Reson Imaging. 2011;29(1):106–10.
88. Villers A, Puech P, Mouton D, Leroy X, Ballereau C, Lemaitre L. Dynamic contrast enhanced, pelvic phased array magnetic resonance imaging of localized prostate cancer for predicting tumor volume: correlation with radical prostatectomy findings. J Urol. 2006;176(6 Pt 1):2432–7.
89. Pepe P, Garufi A, Priolo G, Dibenedetto G, Salemi M, Pennisi M, et al. Accuracy of 3 tesla pelvic phased-array multiparametric mri in diagnosing prostate cancer at repeat biopsy. Arch Ital Urol Androl. 2014;86(4):336–9.
90. Grey AD, Chana MS, Popert R, Wolfe K, Liyanage SH, Acher PL. Diagnostic accuracy of magnetic resonance imaging (MRI) prostate imaging reporting and data system (PI-RADS) scoring in a transperineal prostate biopsy setting. BJU Int. 2015;115(5):728–35.
91. Abd-Alazeez M, Ahmed HU, Arya M, Charman SC, Anastasiadis E, Freeman A, et al. The accuracy of multiparametric MRI in men with negative biopsy and elevated PSA level–can it rule out clinically significant prostate cancer? Urol Oncol. 2014;32(1):45 e17–22.
92. Arumainayagam N, Ahmed HU, Moore CM, Freeman A, Allen C, Sohaib SA, et al. Multiparametric mr imaging for detection of clinically significant prostate cancer: a validation cohort study with transperineal template prostate mapping as the reference standard. Radiology. 2013;268(3):761–9.
93. Priester A, Natarajan S, Khoshnoodi P, Margolis DJ, Raman SS, Reiter RE, et al. MRI underestimation of prostate cancer geometry: use of patient-specific molds to correlate images with whole-mount pathology. J Urol. 2016; doi:10.1016/j.juro.2016.07.084.